SPECTRAL MEASUREMENTS OF WATER PARTICLE VELOCITIES UNDER WAVES

Michael William Bordy

NAVAL POSTGRADUATE SCHOOL
Monterey, California

THESIS

SPECTRAL MEASUREMENTS

OF

WATER PARTICLE VELOCITIES UNDER WAVES

by

Michael William Bordy

Thesis Advisor: E. B. Thornton

March 1972

Spectral Measurements

of

Water Particle Velocities Under Waves

by

Michael William Bordy
Lieutenant, United States Navy
B.S., United States Naval Academy, 1965

Submitted in partial fulfillment of the
requirements for the degree of

MASTER OF SCIENCE IN OCEANOGRAPHY

from the

NAVAL POSTGRADUATE SCHOOL
March 1972

ABSTRACT

Simultaneous measurements of the instantaneous sea surface elevation and water particle velocities were made using a wave staff and an electromagnetic current meter. Measurements were made at three elevations in 18 meters of water at an open ocean site during moderate wave and wind conditions. Coherence of the wave height and orbital velocities was computed to be greater than 0.90 through the range of significant energy-density between 0.05 and 0.22 Hertz. This range contained greater than 90 percent of the total spectral energy-density which indicated that the water particle velocities were almost totally wave-induced. Measured velocity energy-density spectra were compared to theoretically computed spectra using linear wave theory formulation. The measured spectra were 27 to 45 percent greater than theoretical spectra indicating that measured velocities were 5 to 7 percent greater than the theoretical value. Phase spectra were computed for the measured wave heights and orbital velocities. They compared reasonably with first order wave theory.

TABLE OF CONTENTS

LIST OF FIGURES

Figure

Figure

LIST OF SYMBOLS

a	wave amplitude
B	magnetic field intensity
C	degrees centigrade
$C_{12}(f)$	co-spectrum
E	induced electric potential
f	frequency
g	acceleration of gravity
h	total water depth
i	square root of -1
k	wave number
L	wave length
m	meter
$P(_\tau)$	Parzen window function
$Q_{12}(f)$	quadrature spectrum
t	time
u	horizontal component of orbital velocity
v	horizontal component of orbital velocity orthogonal to u
w	vertical component of orbital velocity
W	amplitude of vertical orbital velocity
x	horizontal coordinate
z	vertical coordinate
γ^2	coherence function
Δ	incremental difference
ε	phase angle
σ	angular wave frequency

τ lag time

$\phi_{11}(\tau)$ auto-correlation function

$\phi_{12}(\tau)$ cross-correlation function

$\Phi_{11}(f)$ auto-spectrum

$\Phi_{12}(f)$ cross-sectrum

I. INTRODUCTION

A. BACKGROUND

Measuring instantaneous water particle velocities in the presence of wave-induced motion has been difficult due, primarily, to a lack of instrumentation. This is particularly true for measurements made in the field. Velocity meters must have a high response time, be rugged to operate under wave conditions, and have good directional characteristics, besides the usual requirements of being reliable and accurate. Inman and Nasu (1956) made one of the earliest attempts at field measurements. They used a force meter in shallow water and compared their results to solitary wave theory. Miller and Zeigler (1964) used both an acoustic meter (based on the doppler shift principle) and an electromagnetic flow meter to measure water particle motion in the surf zone. They compared their measurements to high-order wave theory. Nagata (1963, 1964a, 1964b) used an electromagnetic flow meter in a series of experiments to measure water particle velocities in the surf zone and to determine wave directional spectra. Bowden and Fairbairn (1956), Bowden and White (1966), and Simpson (1968), used an electromagnetic flow meter developed at the National Institute of Oceanography.

Simpson's experiments were performed at an open coastal site. He employed spectral methods in the analysis of the orbital velocities and wave height records. The attenuation

of waves with depth determined from the ratios of surface elevation and pressure spectra, and the ratios of the velocity and pressure spectra were found to be consistant with linear wave theory.

Seitz (1971) measured vector water velocities and sea surface displacement at a depth of one meter in an esturary and compared the measured velocity spectra to a derived velocity spectra obtained from direct measurement of the surface wave field. The conclusions drawn were that the direct measurement of the velocity components yielded energy spectra that could be separated into a component due to background turbulent energy and a second component due to surface wave induced velocities. Thus the total water particle motion at depth can be described as the sum of the turbulent velocities and the surface wave-induced motion.

B. RESEARCH OBJECTIVE

The scope of this investigation was divided into three phases:

1. Simultaneous measurements of the instantaneous water particle velocity and sea surface elevation were conducted at an open ocean site in intermediate water depth employing an electromagnetic current meter and wave staff system;
2. Spectral analysis was performed on the wave and velocity records to obtain the statistical properties of the data;

3. First order wave theory was employed to describe the wave and water particle motion spectra and to compare the measured results with the theoretically predicted values.

II. THEORETICAL CONSIDERATIONS

A. FIRST ORDER WAVE THEORY AND SUPERPOSITION

The linearity of first order wave theory permits the utilization of the principle of superposition whereby a random sea surface may be expressed as a summation of an infinite number of small amplitude progressive waves.

$$\eta_{total} = \eta_T = \eta_1 + \eta_2 + \eta_3 + \cdots + \eta_n \qquad (2.1)$$

Using the first order expression for η_T

$$\eta_T = \sum_{n=1}^{\infty} a_n \sin (k_n x - \sigma_n t + \varepsilon_n) \qquad (2.2)$$

where a is the wave component amplitude, k is the wave number, σ is the radial frequency, ε is an arbitrary phase angle, and n is the nth harmonic.

First order (Airy) wave theory can be used to predict the water particle motion under the wave surface. The water particle velocities are described as a linear process and therefore are subject to superposition. For horizontal motion the expression is

$$u_T(t) = \sum_{n=1}^{\infty} \frac{a_n g\, k_n \cosh k_n(h+z)}{\sigma_n \cosh k_n h} \sin(k_n x - \sigma t + \varepsilon_n) \qquad (2.3)$$

where h is the total water depth and z is the vertical coordinate measured positively upward from the surface. For vertical motion the expression is

$$w_T(t) = \sum_{n=1}^{\infty} \frac{a_n g\, k_n \sinh k_n(h+z)}{\sigma_n \cosh k_n h} \cos(k_n x - \sigma t + \varepsilon_n) \qquad (2.4)$$

B. LIMITATIONS OF FIRST ORDER WAVE THEORY

First order wave theory assumes an inviscid and incompressible fluid, irrotational flow and that the wave steepness ratio, a/L (amplitude to wave length), is very small. While a slightly more accurate representation of a random sea surface can be obtained using higher order theory, the non-linearity of these theories does not permit superposition of solutions to the wave equation. This in turn precludes analysis by spectral methods.

First order theory can provide a good approximation to the wave processes for small to moderate conditions. Dean (1968) compared various wave theories and how well they fitted the dynamic and kinematic free surface boundary conditions. He showed that for waves with profiles having small values of slope in intermediate water depths, first order theory provides one of the better solutions to the wave equation. These two conditions were satisfied in this study which lends validity to the analysis performed.

III. INSTRUMENTATION

The water particle velocities were measured with an Engineering Physics Company water current meter Model EMCM-3B. The sea surface elevation was measured with a Baylor Company wave staff system Model 13528.

A. WATER CURRENT METER

The EMCM-3B is an electromagnetic current measuring device which measures two orthogonal components of water particle velocity through a range of from zero to five meters per second. Two d.c. voltage signals proportional to the magnitude of the orthogonal velocity components are produced. The minimum electrical response time of the system is 0.2 seconds corresponding to frequency measurements of 5 Hertz. The output rms noise level is a function of the output time constant. A maximum noise level of 22.4 millivolts (-16db) occurs at a frequency of 5 Hertz. The maximum output error is one percent of full scale reading. The transducer is made of a fiberglass material. The dimensions of the transducer are 2-3/4 inches in diameter and 36 inches in length.

The current meter operates by Faraday's principle of magnetic induction. A toroidal magnet imbedded in the cylindrical transducer produces a magnetic field in the water. The intensity of the field decreases according to the inverse square law. A potential distribution is

produced in the water flowing through the field and is sensed by two pairs of electrodes on the face of the transducer. The vector equation is

$$\vec{E} = \vec{u} \times \vec{B} \qquad (3.1)$$

where $\vec{E}$ is the induced electric potential, $\vec{u}$ is the velocity of the motion, and $\vec{B}$ is the intensity of the magnetic field. It has been established that the magnitude of the induced potential $\vec{E}$ is independent of the conductivity of the metered fluid provided the conductivity is above a threshold value of 10^{-5} mhos per meter of fluid. Both fresh and salt water have conductivities several orders of magnitude above this threshold. The direction of the flow is indicated by a reversal of the polarity of the induced potential $\vec{E}$ when the flow reverses.

The transducer senses the motion of the fluid in an area approximately two to three probe radii from the sensor. This limits the spatial resolution to approximately six times the diameter or 42 centimeters. A spatial resolution places a limitation on the frequency resolution. A wave having a wave length in deep water of 42 centimeters corresponds to approximately a 0.5 second period wave. This limits the frequency resolution to 2 Hertz.

To increase the frequency resolution, it is necessary to use a smaller diameter transducer. The spatial resolution is the limitation of the response of electromagnetic flow meters as it is for other meters based on doppler shift or back scatter of acoustic or electromagnetic (laser) waves.

B. WAVE STAFF SYSTEM

The Baylor Model 13528 is a wave profile recording system which measures instantaneous sea surface elevation as a function of time. Measurements are accurate within one percent of actual height. The system consists of three components, the wave staff, transducer, and recorder. The staff is constructed of two wire ropes held parallel by tension and spaced about nine inches apart. The staff is installed perpendicular to the water surface and is stretched with sufficient tension to resist movement due to wind and wave forces.

The transducer unit measures the electrical resistance of the length of the staff above a short circuit between the elements of the staff produced by the motion of the conducting salt water of the sea's surface. A direct current voltage proportional to the height of the sea surface is taken across this fluctuating resistance.

IV. DATA PROCUREMENT AND PRE-PROCESSING

A. DATA PROCUREMENT

Experiments were conducted at the Naval Undersea Research and Development Center Oceanographic Research Tower at San Diego, California, 21 October 1971. The tower is approximately one mile off Mission Beach in a mean water depth of 17 meters. The structure is of steel and concrete and is built into the sea floor. The sides of the tower are inclined at an angle of five degrees from the vertical. An enclosed upper deck houses electronic equipment while an open lower deck provides a working area to place instruments in the water.

Winch controlled instrument carriages which travel on rails down the sides of the tower to about one meter above the sea floor are located on the north, south, and west sides of the tower. The carriages may be placed at any depth for data collection.

The Baylor wave staff is installed on the west side of the tower adjacent to the carriage rails. The west carriage was chosen for placement of the current meter transducer due to the location of the wave staff and to the exposure of that side to the open sea and predominant swell.

The current meter was installed on the carriage as shown in Figs. (1) and (2). With the transducer mounted vertically, two orthogonal components of the horizontal velocity field are measured. When the transducer is mounted horizontally, the total vertical field and one component of the horizontal field is measured.

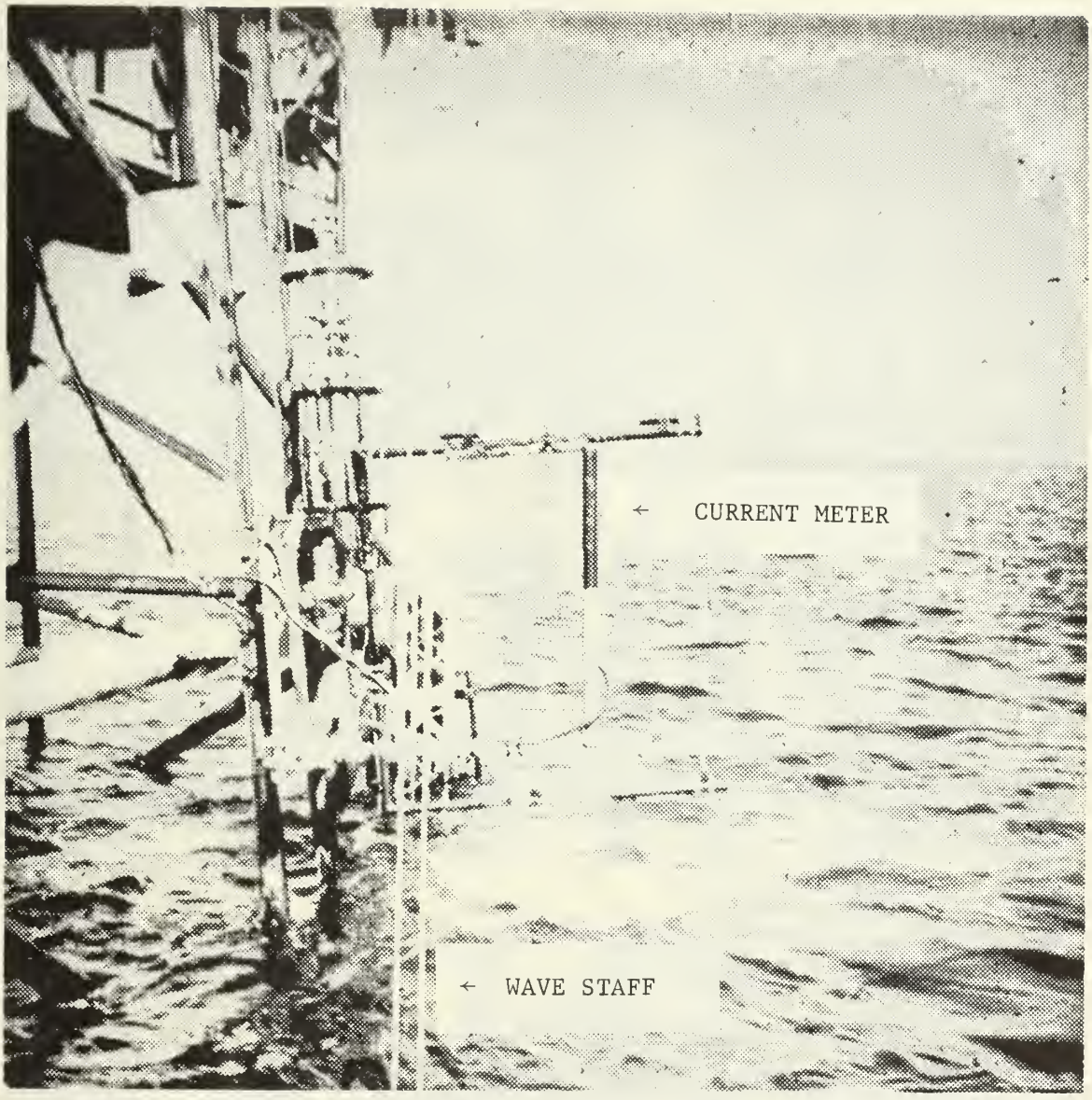

Figure 1. EMCM-3B water current meter mounted to measure orthogonal components of the horizontal velocity field. The Baylor wave staff is to the left of the water current meter transducer.

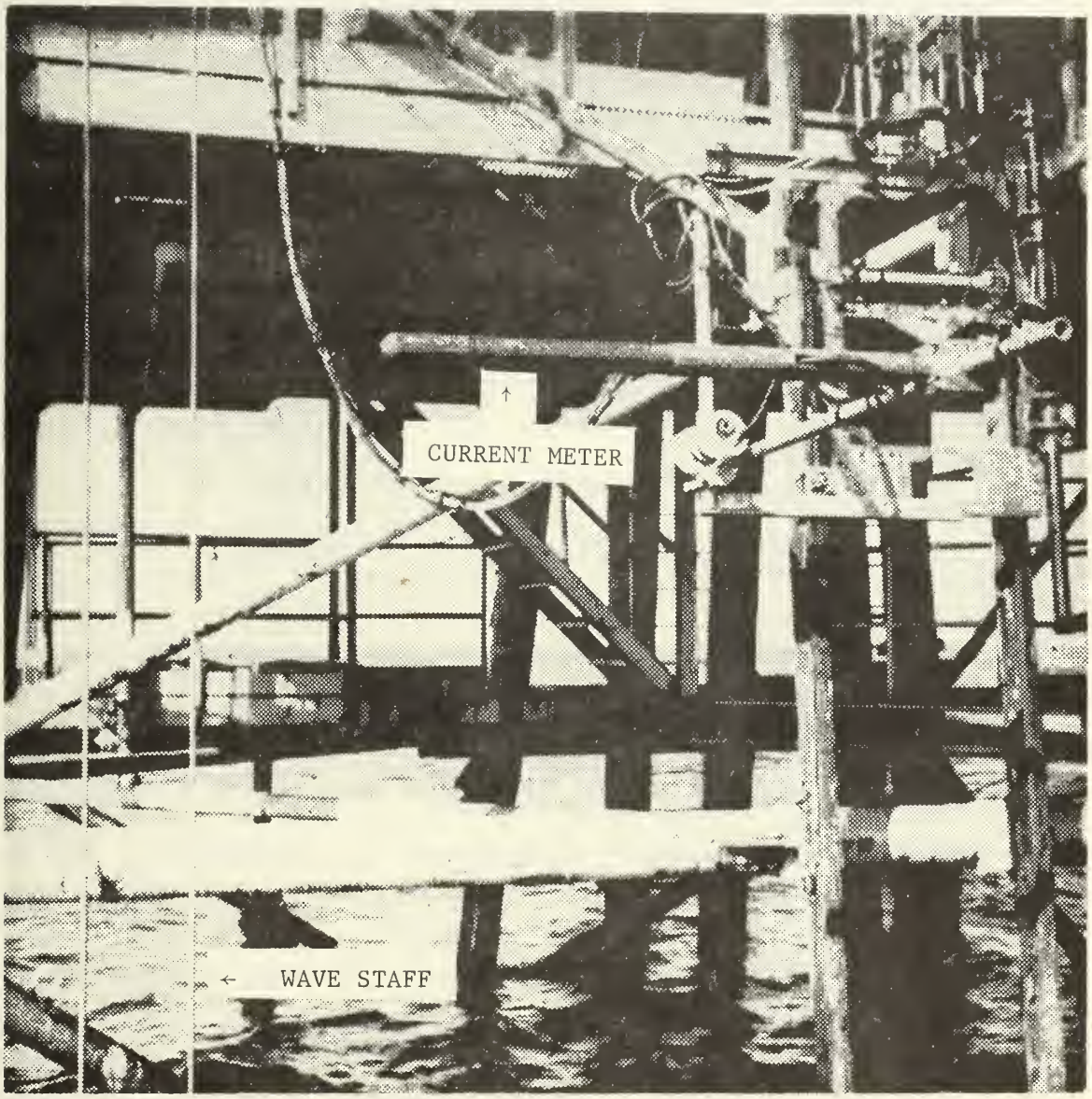

Figure 2. EMCM-3B water current meter mounted to measure total vertical velocity and u component of horizontal velocity. The Baylor wave staff is to the left of the water current meter transducer.

Data chosen for analysis were taken during 4 recording periods each of 20 minutes duration. The instrument depths z(m), height of water column h(m), and velocity components measured for each recording period are summarized in Table I.

TABLE I

RUN	h(m) depth	z(m) instrument depth	COMPONENT
1	18.15	4.12	u & v
2	18.15	5.34	u & w
3	18.15	8.35	u & w
4	18.00	10.00	u & w

The current meter transducer was oriented to measure the u-component of horizontal velocity at an azmiuth of 270° true and the v-component of horizontal velocity at an azmiuth of 360° true.

Throughout the recording time a bi-modal surface swell of about 0.3 meters height was visually observed with one component having a period of about 7 seconds from 285° true, and the other component with a period of about 5 seconds from 260° true. The surface was observed to be non-breaking with a wind capillary system present. The wind was from 310° true at a speed of about 8 knots. A moderate temperature gradient was present with a temperature of 17.5°C at the surface decreasing to 15.0°C at a depth of 18 meters.

B. DATA PRE-PROCESSING

The velocity and wave height data were simultaneously recorded on a Sangamo Model 3500, 14 channel FM tape recorder. The taped data were transcribed to a rectilinear eight channel Clevite Brush recorder after amplification by a Krohn-Hite Model 3322 variable filter. The filter was operated in the 20 decibel gain, low pass, maximally flat mode with a cutoff frequency of 99.9 Khz. This resulted in a gain of ten with no filtering or phase shift.

The two velocity components and the wave height were simultaneously recorded on adjacent channels of the brush recorder (Fig. 3) to conserve phase relationships during the digitizing process.

A Calma Company Model 480 mechanical digitizer was used to digitize the continuous strip chart information at 100 points to the inch. This corresponded to a sampling interval of 0.2032 seconds. The digitized records were interpreted by program CONVERT (Lynch, 1970) using the CDC 6500 computer at the Fleet Numerical Weather Central, Monterey.

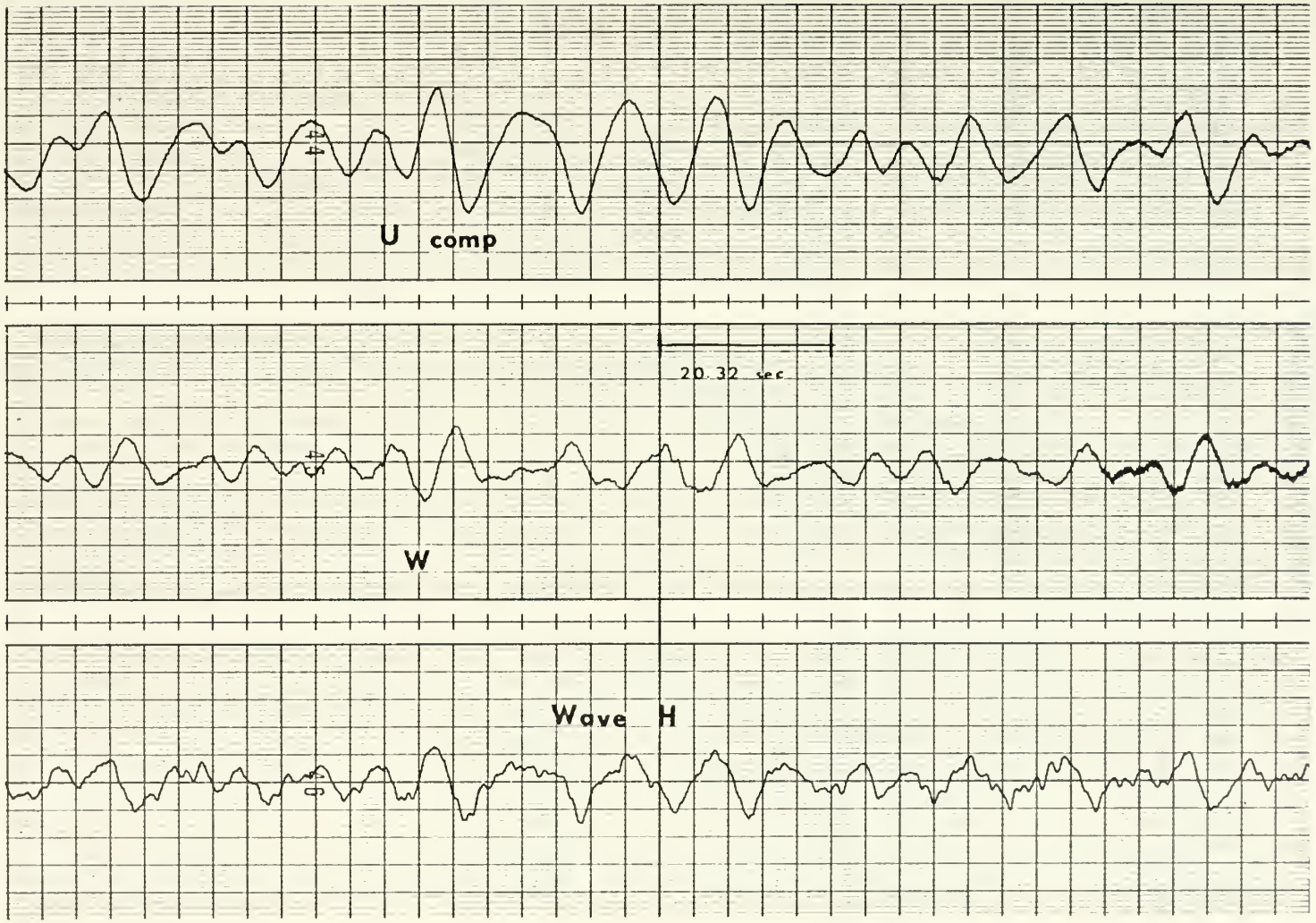

Figure 3. Strip chart record of u-component horizontal velocity w-component of vertical velocity and Baylor wave height.

V. SPECTRAL ANALYSIS

Analysis of the digitized records was performed on an IBM 360 digital computer in accordance with the methods of Blackman and Tukey (1958).

A. COMPUTATION OF THE ENERGY-DENSITY SPECTRUM

The energy-density spectrum is computed from the Fourier transform of the auto-correlation function of the record time series. The auto-correlation function expressed as a function of lag time τ, is defined as

$$\phi_{11}(\tau) = \lim_{T \to \infty} \frac{1}{T} \int_{t}^{t+T} x_1(t) x_1(t+\tau)\, dt \qquad (5.1)$$

where $x_1(t)$ represents the time series being analyzed. The Fourier transform is

$$\Phi_{11}(f) = \lim_{T \to \infty} \frac{1}{T} \int_{-\frac{T}{2}}^{\frac{T}{2}} \phi_{11}(\tau) e^{-i2\pi f \tau}\, d\tau \qquad (5.2)$$

A Parzen lag window was applied to the correlation functions to account for the finite length of the records in computing the spectra. The Parzen window has the desirable property of no negative side lobes. This eliminates any numerical instability problems that may arise in the analysis procedure. The Parzen window function is defined between the limits of $\pm$ Tm/2 as

$$P(\tau) = \begin{cases} \left[1 - 6\frac{\tau}{Tm}\right]^2 \left[1 - \frac{|\tau|}{Tm}\right] & |\tau| \leq \frac{Tm}{2} \\ 2\left[1 - \frac{\tau}{Tm}\right]^2 & |\tau| \geq \frac{Tm}{2} \end{cases} \qquad (5.3)$$

where Tm = total lag time. The Fourier transform function of the modified auto-correlation function is

$$\Phi'_{11}(f) = \int_{-\infty}^{\infty} P(\tau)\, \phi_{11}(\tau) e^{-i2\pi f\tau}\, d\tau \qquad (5.4)$$

The energy-density spectrum is the statistical estimate of the energy-density distribution in the frequency bands comprising the spectrum. The area under the curve of the wave height spectrum is proportional to the total potential energy-density of the sea surface elevation. The area under the curve of the velocity spectrum is proportional to the total kinetic energy-density. In both instances, the area under the curve is equal to twice the variance of the random variable.

B. COMPUTATION OF THE CROSS-SPECTRAL DENSITY

The cross-spectral density is defined as the Fourier transform of the cross-correlation function. The lag window considerations are identical to those for the energy-density spectrum described above. The cross-correlation function is similar to the auto-correlation function except that a second time series record is lagged against the first instead of a single record lagged against itself. The cross-correlation function indicates the dependence of values of one

record on values of the second record for various values of lag time. The time averaged cross-correlation function is defined as

$$\phi_{12}(\tau) = \lim_{T\to\infty} \frac{1}{T} \int_{-\frac{T}{2}}^{\frac{T}{2}} x_1(t)x_2(t+\tau)\, dt \qquad (5.5)$$

and the cross-spectral density is

$$\Phi_{12}(f) = \int_{-\infty}^{\infty} P(\tau)\, \phi_{12}(\tau)e^{-i2\pi f\tau}\, d\tau \qquad (5.6)$$

where $P(\tau)$ is the Parzen function defined above. The cross-spectrum can be defined in terms of its real and imaginary parts

$$\Phi_{12}(f) = C_{12}(f) - i\, Q_{12}(f) \qquad (5.7)$$

where the real part of $\Phi_{12}(f)$ is the co-spectrum

$$C_{12}(f) = 2 \int_{0}^{\infty} [\phi_{12}(\tau) + \phi_{12}(-\tau)] \cos(2\pi f\tau)\, d\tau \qquad (5.8)$$

and the imaginary part of $\Phi_{12}(f)$ is the Quadrature spectrum

$$Q_{12}(f) = 2 \int_{0}^{\infty} [\phi_{12}(\tau) - \phi_{12}(-\tau)] \sin(2\pi f\tau)\, d\tau \qquad (5.9)$$

C. COMPUTATION OF PHASE ANGLE

The phase angle of the cross spectral density is a useful tool in analysis of bivariate systems. The spectral phase angle represents the average angular difference by which the

cross correlated components of $x_2(t)$ lead those of $x_1(t)$ in each spectral frequency band. The phase angle of the cross spectral density is

$$\varepsilon_{12}(f) = \arctan\left[\frac{Q_{12}(f)}{C_{12}(f)}\right] \tag{5.10}$$

where $Q_{12}(f)$ and $C_{12}(f)$ are defined above. $\varepsilon_{12}(f)$ spans the values

$$-180^{o} \leq \varepsilon_{12}(f) \leq 180^{o}. \tag{5.11}$$

D. COMPUTATION OF COHERENCY

The coherency spectrum provides a non-dimensional measure of the correlation between two time series as a function of frequency. The coherence function is defined as

$$\gamma^2_{12}(f) = \frac{\left[\Phi_{12}(f)\right]^2}{\Phi_{11}(f)\ \Phi_{22}(f)} \tag{5.12}$$

The cross spectral density function $\Phi_{12}(f)$ satisfies the inequality

$$|\Phi_{12}(f)|^2 \leq \Phi_{11}(f)\ \Phi_{22}(f) \tag{5.13}$$

which implies that

$$0 \leq \gamma^2(f) \leq 1 \tag{5.14}$$

For an idealized constant parameter linear system with clearly defined input and output, the coherence function will be equal to unity. Bendat and Piersol (1966) attribute coherency values greater than zero but less than unity

to three possible causes; the system is not linear, extraneous noise is present in the measurements, or the output response is due to more than one input function.

VI. ANALYSIS OF DATA

The data was sampled at 0.2032 second intervals which gives a Nyquist frequency of 2.46 Hertz. This was sufficiently high to avoid aliasing problems. The maximum lag time was chosen as 10 percent of the record length which were 20 minutes each. This gives a frequency resolution of 0.0042 Hertz.

A. HORIZONTAL VELOCITY MEASUREMENTS

The predicted and measured horizontal velocity spectra, the phase angle and the coherence of the wave height and u-component velocity were computed during run number 1. The total depth of water was 18.15 meters and the velocity meter was at a depth of 4.12 meters.

1. Predicted and Measured Horizontal Velocity Spectra

The energy-density spectrum of the predicted horizontal velocity was calculated from the wave-induced horizontal velocity field derived from the expression

$$|u(f)|^2 = \left[\frac{f \cosh k(h+z)}{2\pi \sinh kh}\right]^2 |\eta(f)|^2 \qquad (6.1)$$

The term in brackets is the first order velocity amplitude response function squared. The measured total horizontal velocity energy-density spectrum was formed by computing the energy-density spectra of the measured u and v orthogonal velocity components and summing the spectra across the spectral frequency band.

The energy-density spectra, Fig. (4), have approximately the same shape between 0.05 to 0.35 Hertz with the measured spectrum slightly wider than the predicted spectrum. The measured spectrum is from 30 to 50 percent greater than the predicted spectrum across the spectral band width of significant energy.

2. Coherence

The theoretical coherence between two ideally correlated records is 1.0. The coherence of the measured wave and u-component velocity is greater than 0.90 in the frequency band of 0.05 to 0.22 Hertz, Fig. (5). This frequency band contains greater than 90 percent of the total energy-density in the spectra, and will be referred to henceforth as the band width of significant energy-density. The high coherence between the wave and velocity spectra indicates the instantaneous velocities are primarily wave induced over the region of significant energy-density, and the incoherent (turbulent) energy contribution to the spectrum is small.

3. Phase Angle

The theoretical phase angle between the instantaneous wave height and wave induced u-component of velocity is zero degrees. The computed phase angle ranges from 10 to 70 degrees across the band of high coherence with low values of phase angle at low frequencies increasing to larger values at the higher frequencies, (See Fig. (6)).

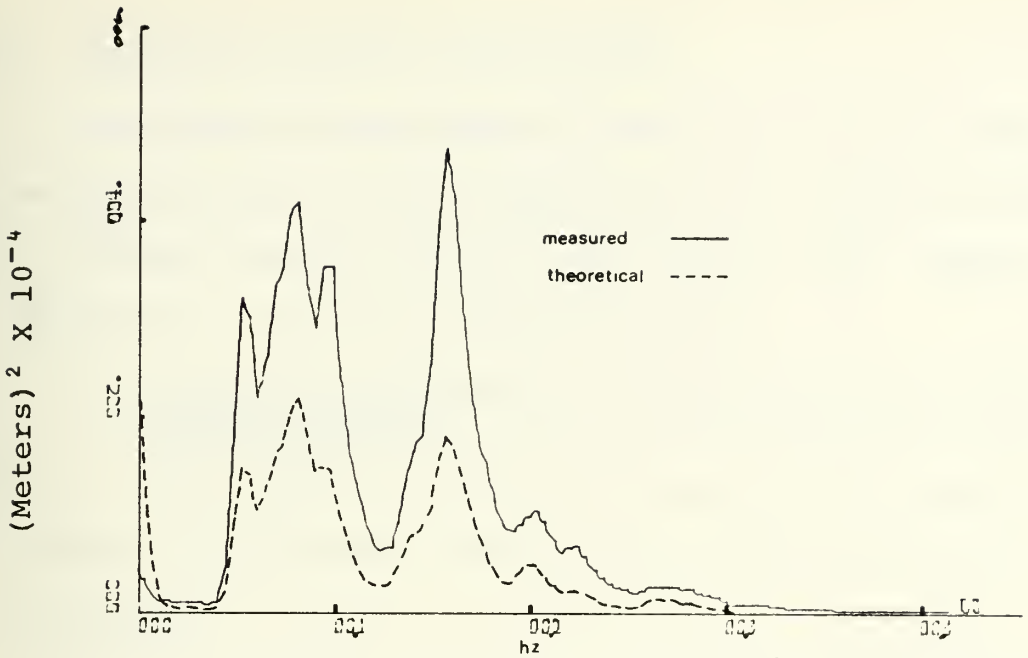

Figure 4. Measured and Theoretical Horizontal Velocity Spectra. Depth 4.12 Meters, 21 October 1971.

Figure 5. Coherence of Wave Height and u-Component of Horizontal Velocity. Depth 4.12 Meters, 21 October 1971.

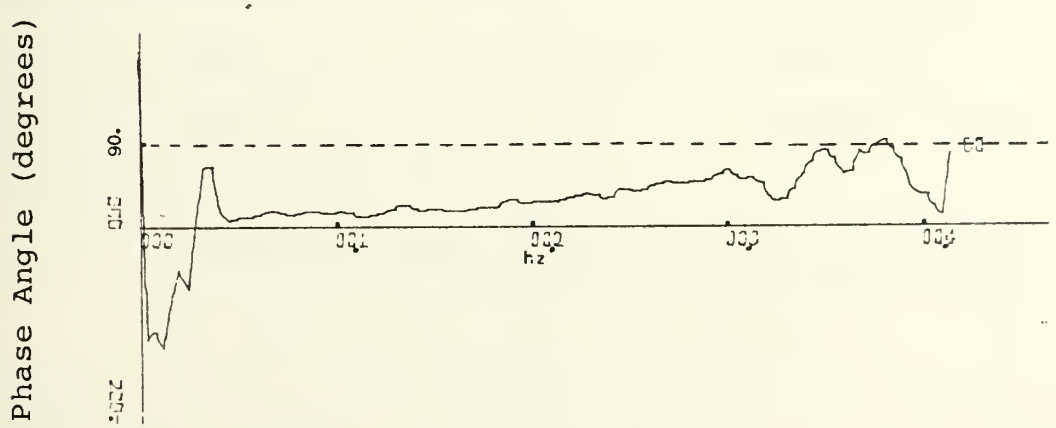

Figure 6. Phase Angle of Wave Height and u-Component of Horizontal Velocity. Depth 4.12 Meters, 21 October 1971.

B. VERTICAL VELOCITY MEASUREMENTS

The predicted and measured vertical velocity energy-density spectra, and the phase angle and coherence spectra of the wave height and vertical velocity were computed for depths of 5.34, 8.35, and 10.00 meters.

1. Predicted and Measured Vertical Velocity Energy-Density Spectra

The predicted vertical velocity energy-density spectrum was computed from the wave spectrum using the expression

$$|w(f)|^2 = \left[\frac{f}{2\pi} \frac{\sinh k(h+z)}{\sinh kh}\right]^2 |\eta(f)|^2 \qquad (6.2)$$

The term in brackets is the first order vertical velocity amplitude response function squared.

The predicted and measured energy-density spectra are shown in Figs. (7), (10), and (13). The spectral band of significant energy-density is essentially the same for the three depths measured, 0.05 to 0.35 Hertz. The magnitude of the measured energy spectrum is 30 to 50 percent greater than the predicted energy spectrum at each depth. This means that the actual velocities were 5 to 7 percent greater than theoretically predicted values.

2. Coherence of Wave Height and Vertical Velocity

The coherence for each depth are shown in Figs. (9), (12), and (15). The coherence is greater than 0.9 at each of the three depths over the range of significant energy-density. This indicates a high correlation between the wave and wave-induced vertical velocity spectra which means

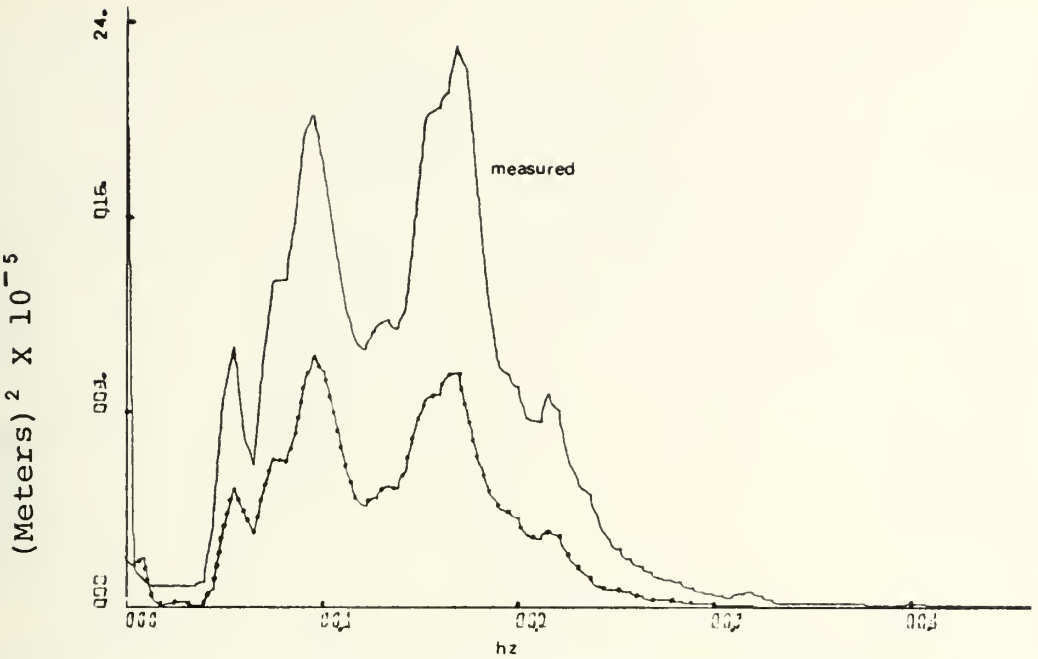

Figure 7. Measured and Theoretical Vertical Velocity Spectra. Depth 5.34 Meters, 21 October 1971.

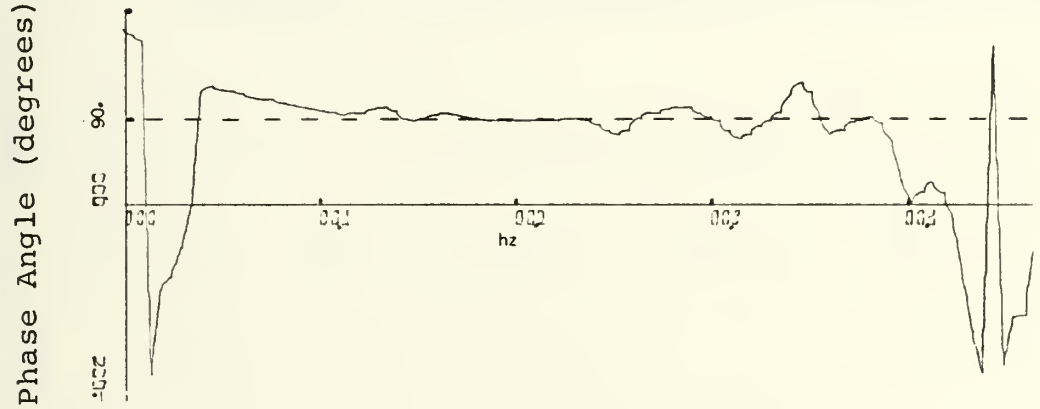

Figure 8. Phase Angle Between Wave Height and Vertical Velocity. Depth 5.34 Meters, 21 October 1971.

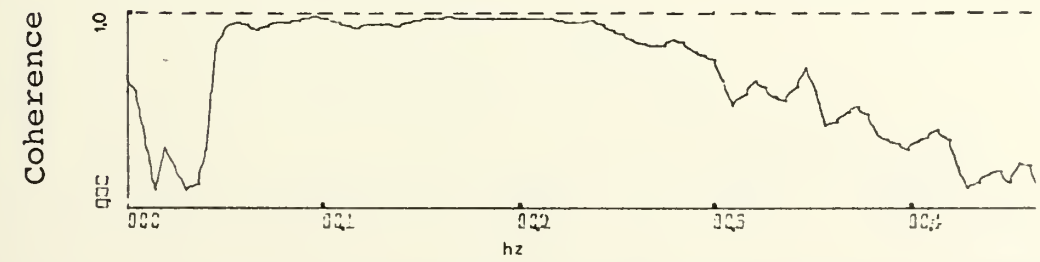

Figure 9. Coherence of Wave Height and Vertical Velocity. Depth 5.34 Meters, 21 October 1971.

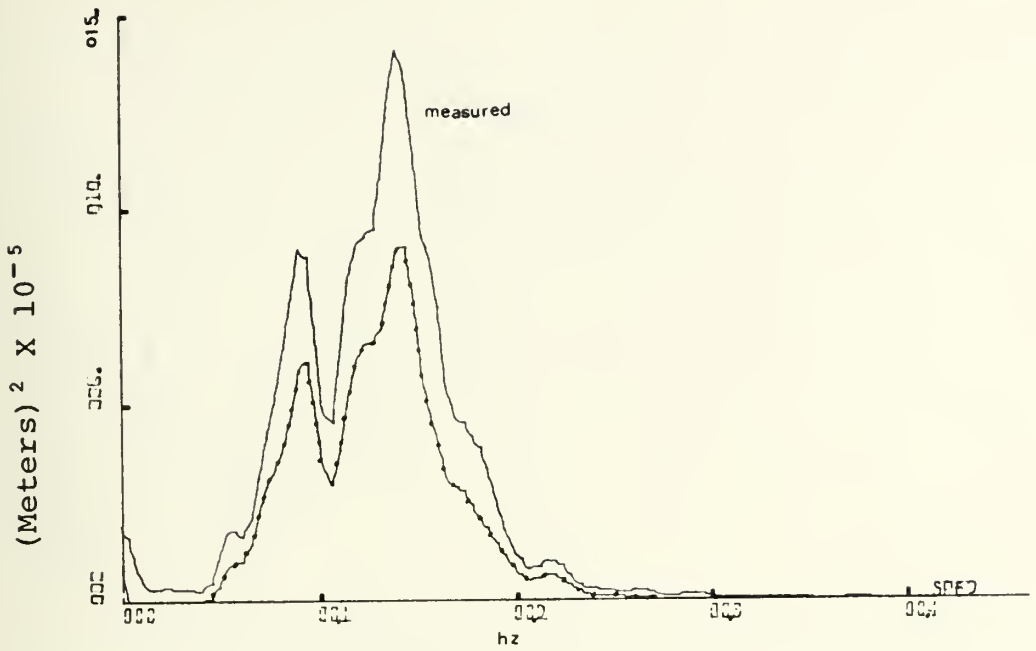

Figure 10. Measured and Theoretical Vertical Velocity Spectra. Depth 8.35 Meters, 21 October 1971.

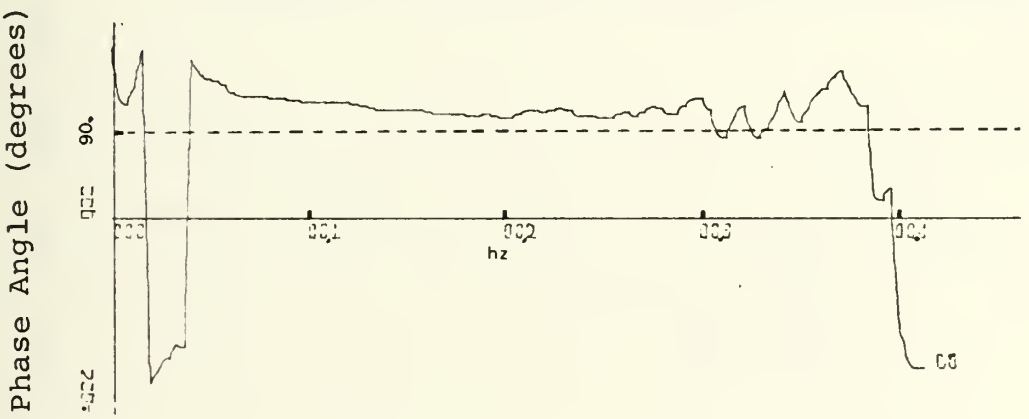

Figure 11. Phase Angle Between Wave Height and Vertical Velocity. Depth 8.35 Meters, 21 October 1971.

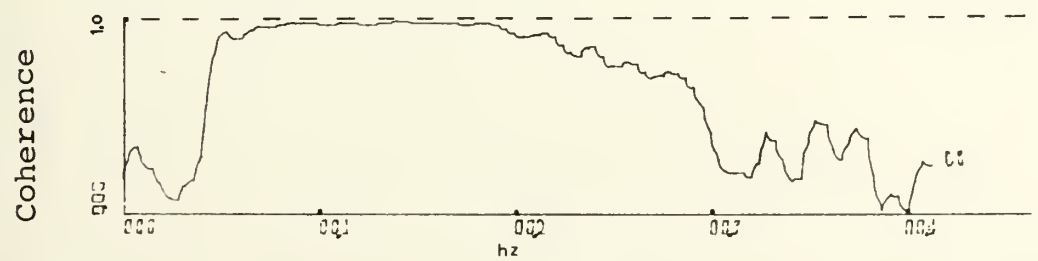

Figure 12. Coherence of Wave Height and Vertical Velocity. Depth 8.35 Meters, 21 October 1971.

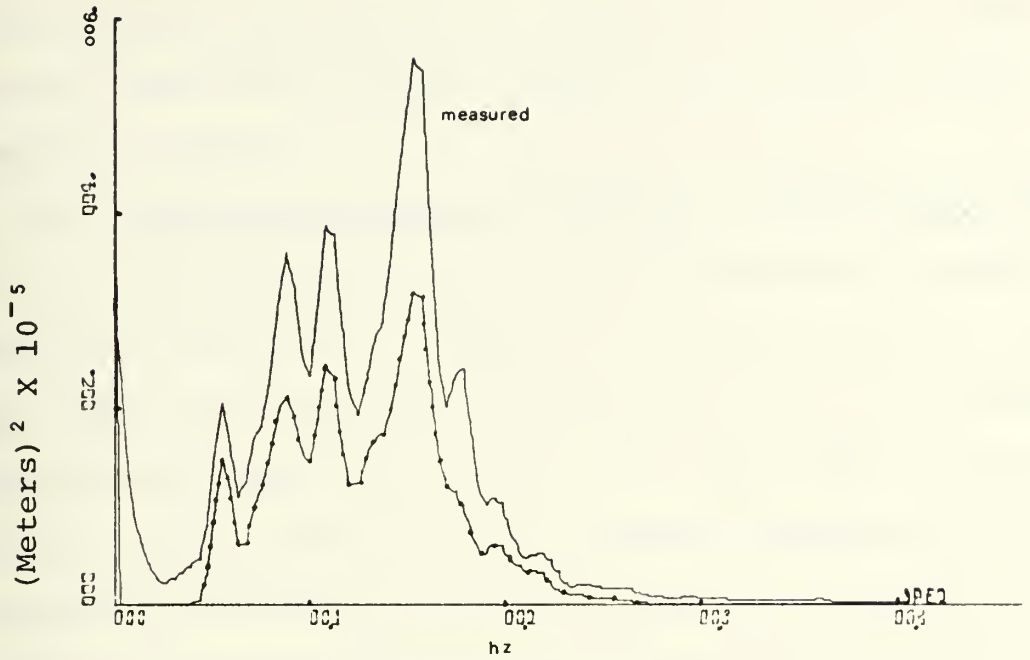

Figure 13. Measured and Theoretical Vertical Velocity Spectra. Depth 10.00 Meters, 21 October 1971.

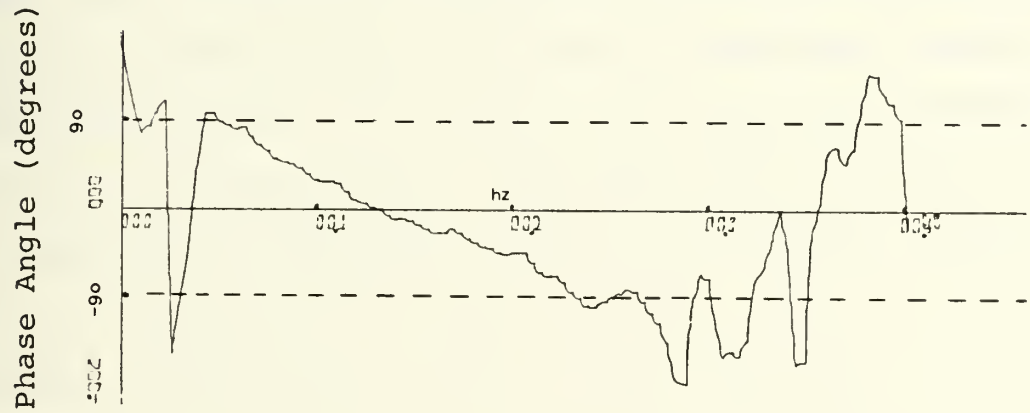

Figure 14. Phase Angle Between Wave Height and Vertical Velocity. Depth 10.00 Meters, 21 October 1971.

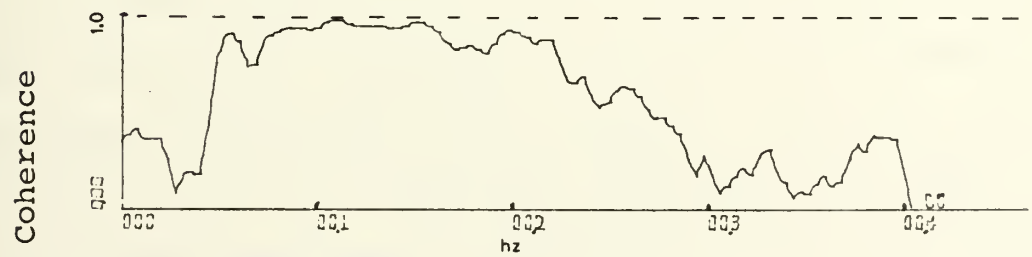

Figure 15. Coherence of Wave Height and Vertical Velocity. Depth 10.00 Meters, 21 October 1971.

that most of the instantaneous measured velocity is due to the waves and turbulent energy contributions to the spectra is small.

3. Phase Angle Between Wave Height and Vertical Velocity

The theoretical phase angle between wave height and vertical velocity is 90 degrees. The measured phase spectrum at a depth of 5.34 meters, shown in Fig. (8), corresponds well to this theoretical value. The phase spectrum at 8.35 meters, shown in Fig. (11), is uniformly greater than 100 degrees and decreases across the band of significant energy-density. The phase spectrum at a depth of 10.00 meters, Fig. (14), shifted from approximately plus 90 degrees to minus 90 degrees across the band of significant energy-density which was not expected. The coherence through this range is uniformly high. This phase shift is partly due to a horizontal displacement of the current meter transducer from a vertical line to the wave staff. This is discussed below, but the shift cannot be fully explained. The 10.00 meter run in which this occurred was measured sequentially between the 5.34 and 8.35 meter runs which did not show a similar phase shift. All three runs were conducted in a two hour period; this tends to discount the possibility of equipment malfunction. This suggests a phase shifting departing from the theoretical increasing with depth, but more experiments need to be conducted before any definite conclusions can be made.

4. Phase Angle Error

The rails on which the instrument carriage was mounted are inclined at an angle of 5 degrees from the vertical. This inclination caused the current meter transducer to be displaced horizontally from a line vertical to the Baylor wave staff at the depths of measurement. The magnitude of this displacement was 0.467, 0.732, and 1.068 meters respectively at the measured depths of 5.34, 8.35, and 10.00 meters. The displacements resulted in a phase error due to the time lag between sensing of the waves by the current meter and the wave staff.

The maximum percentage error was computed by employing the first order expressions for η and the w-component

$$\eta = a \sin(kx-\sigma t) = a \cos\left[90^{o} - (kx-\sigma t)\right] \qquad (6.3)$$

$$w = W \cos(kx-\sigma t) = W \cos\left[180^{o} - (kx-\sigma t)\right] \qquad (6.4)$$

where W is the amplitude of the vertical velocity. The bracketed terms in each expression are the phase angles,

$$\varepsilon_{\eta} = 90^{o} - (kx-\sigma t) \qquad (6.5)$$

and

$$\varepsilon_{w} = 180^{o} - (kx-\sigma t) \; . \qquad (6.6)$$

Using the wave staff as a reference, the x term in ε_{η} is set equal to zero, so that

$$\varepsilon_{\eta} = 90^{o} - \sigma t \qquad (6.7)$$

and the phase difference $\Delta\varepsilon$ is

$$\Delta\varepsilon = \varepsilon_w - \varepsilon_\eta = \Delta\varepsilon = 90^o - kx \qquad (6.8)$$

where x is the horizontal distance between the wave staff and the current meter transducer. If x is equal to zero, the theoretical phase angle of 90^o is obtained.

The percentage error is

$$\text{Percent Error} = \frac{kx}{90}\left(\frac{360}{2\pi}\right) \qquad (6.9)$$

The percent error of the maximum computed phase spectra for each depth has been plotted in Figs. (16), (17), and (18). The amplitudes of the actual phase spectra are smaller than those of the computed phase spectra by the indicated percentage at each frequency. The error is small at low frequencies and increases at the higher frequencies where the ratio of the horizontal displacement of the current meter to the length of the waves is high.

5. Percent Error of Predicted and Measured Energy-Density Spectra

The percentage error of the energy-density spectra for each depth are shown in Figs. (19), (20), and (21). The error rapidly decreases to low values (25 to 50 percent) at low frequencies and remains uniform across the range in which the coherence is high. The average error over the band of significant energy-density was highest (45 percent) for the measurement at 5.34 meters. The average error was approximately the same (30 percent), over the band of significant energy-density for the measurements at 8.35 and 10.00 meters. The actual error between the predicted and measured

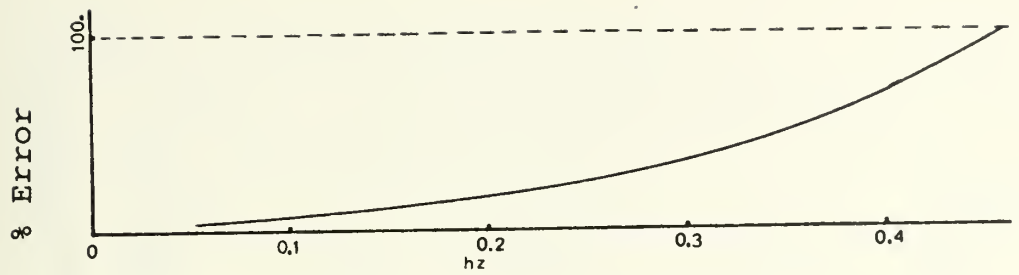

Figure 16. Phase Angle Error Between Wave Height and Vertical Velocity. Depth 5.34 Meters, 21 October 1971.

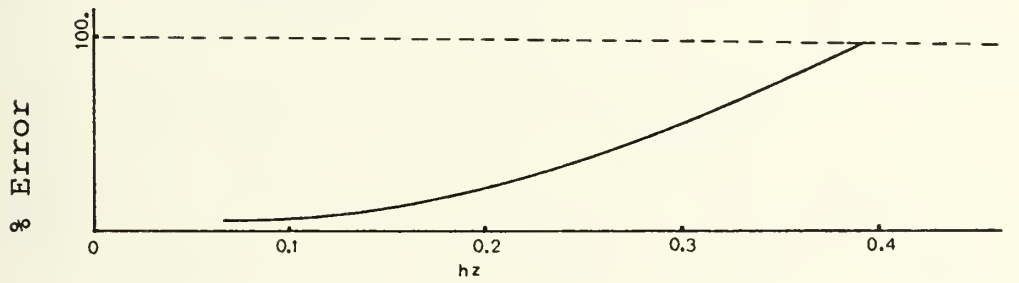

Figure 17. Phase Angle Error Between Wave Height and Vertical Velocity. Depth 8.35 Meters, 21 October 1971.

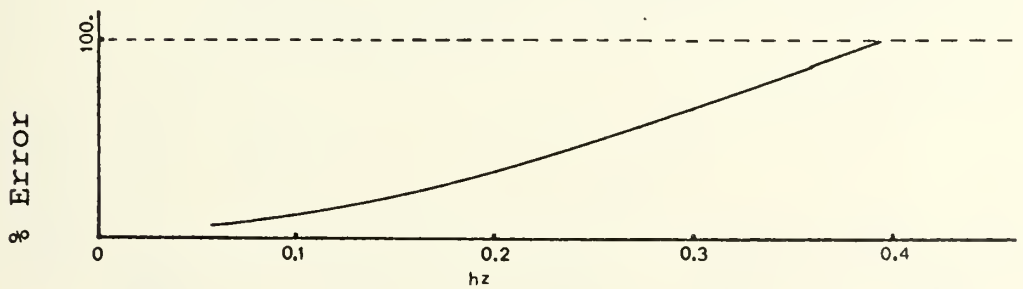

Figure 18. Phase Angle Error Between Wave Height and Vertical Velocity. Depth 10.00 Meters, 21 October 1971.

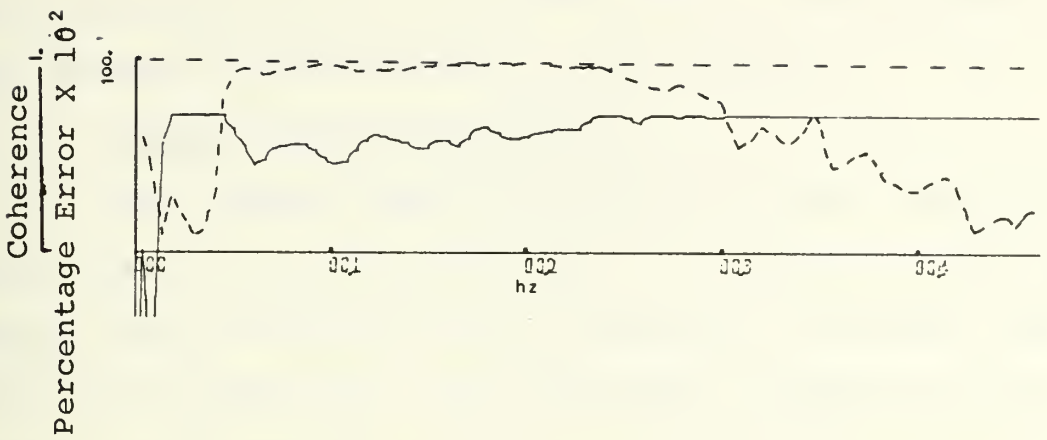

Figure 19. Percent Error of Measured and Theoretical Vertical Velocity Spectra and Coherence (dashed line) of Wave Height and Measured Vertical Velocity. Depth 5.34 Meters, 21 October 1971.

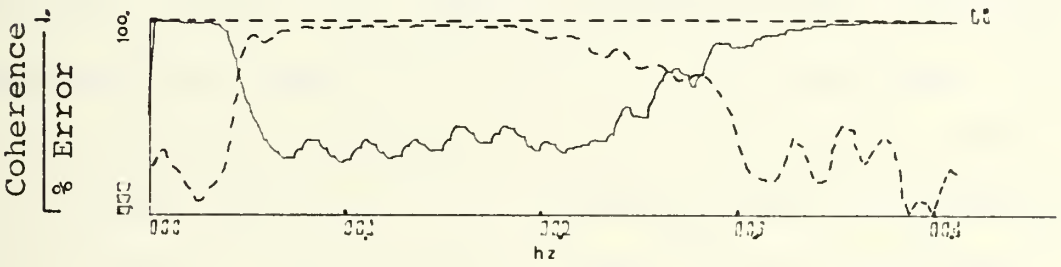

Figure 20. Percentage Error of Measured and Theoretical Vertical Velocity Spectra and Coherence (dashed line) of Wave Height and Measured Vertical Velocity. Depth 8.35 Meters, 21 October 1971.

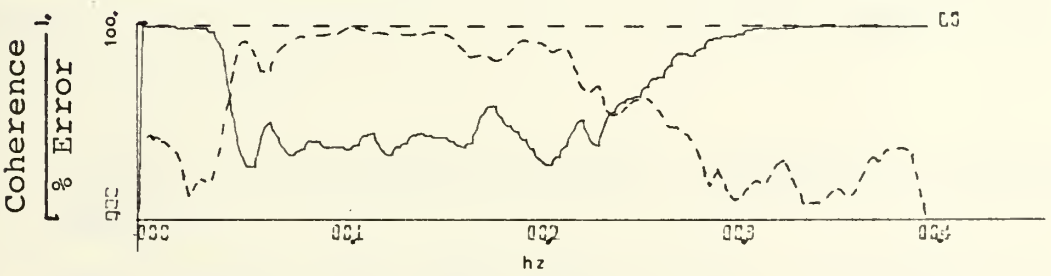

Figure 21. Percentage Error of Measured and Theoretical Vertical Velocity Spectra and Coherence (dashed line) of Wave Height and Measured Vertical Velocity. Depth 10.00 Meters, 21 October 1971.

velocity amplitudes is the square root of these values and amounts to approximately 5 to 7 percent.

6. Current Meter Calibration

The current meter was calibrated under steady flow conditions in a circular tow tank. The boundary layer under steady flow on the face of the transducer is greater than that for unsteady flow. The instrument essentially integrates the intensity of the potential which decreases in intensity as the reciprocal of the square of the distance from the transducer. The steady flow calibration will indicate a faster flow than for unsteady flow. This indicates that the measured flow will be over-predicted. The orbital velocities measured in this investigation were of an unsteady turbulent nature indicating that a calibration error exists. The magnitude of this error is presently unknown. A method of calibrating the current meter under turbulent conditions is currently being developed at the Naval Postgraduate School. Re-calibration under dynamic conditions is expected to reduce the errors computed in this investigation.

C. ANALYSIS OF HORIZONTAL VELOCITY COMPONENT AND VERTICAL VELOCITY

The coherence and phase angle of the u-component of horizontal velocity and the vertical velocity were computed for measurements at depths of 5.34, 8.35, and 10.00 meters and are shown in Figs. (22, (23), and (24).

According to first order wave theory, the horizontal and vertical orbital velocities have a phase angle difference of 90 degrees with the w-component leading the u-component. The theoretical coherence is equal to unity. The computed values for the measurements at 5.34 and 8.35 meters agree quite well with theory. The coherence is 0.9 through the region of significant energy-density. The coherence of the velocities at 10.00 meters is also 0.9 but the phase angle again exhibits peculiar behavior as it did between the wave height and vertical velocity discussed above. More data are required to explain this phenomenon.

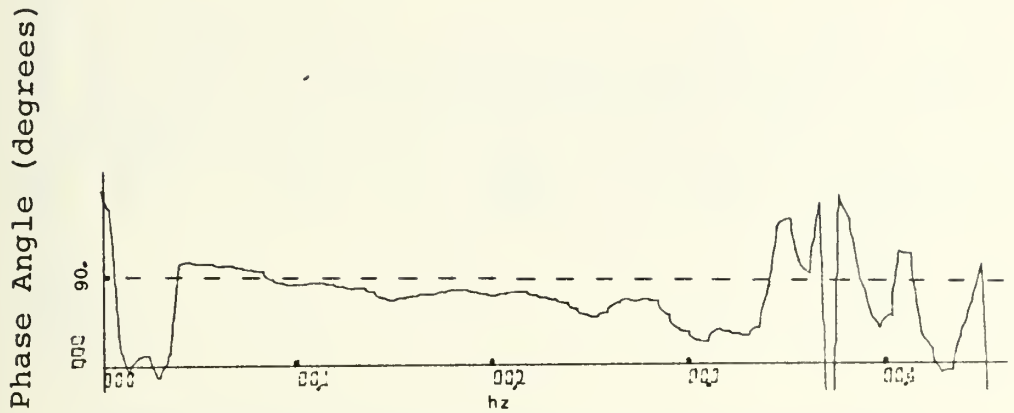

Phase Angle Between Vertical and Horizontal Velocity Component. Depth 5.34 Meters, 21 October 1971.

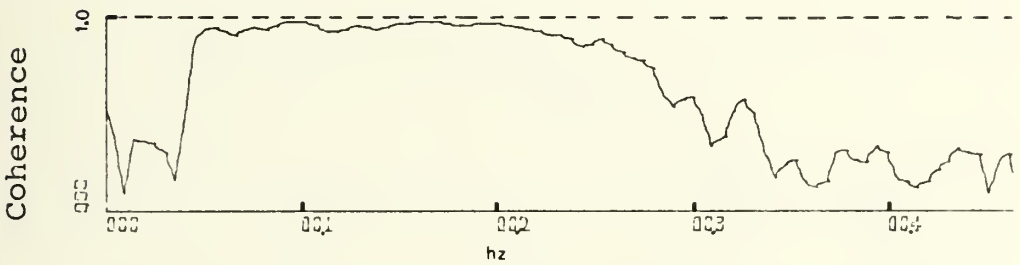

Coherence of Vertical and Horizontal Velocity Component. Depth 5.34 Meters, 21 October 1971.

Figure 22. Phase Angle and Coherence 5.34 Meters 21 October 1971.

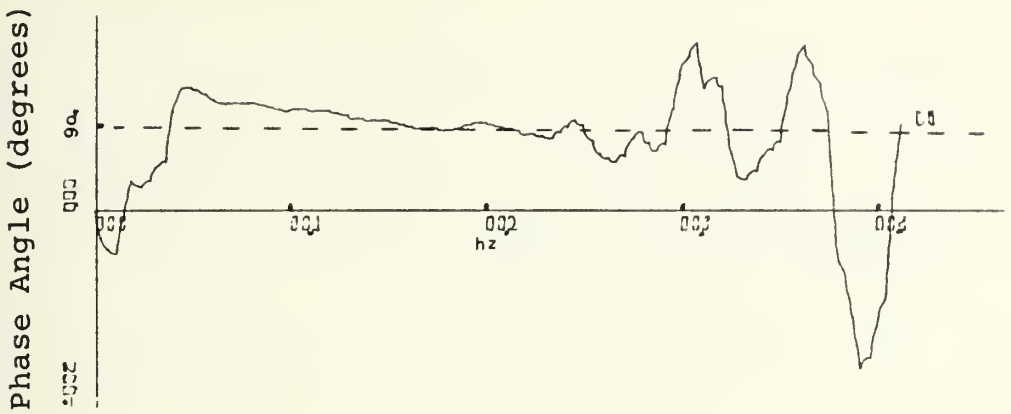

Phase Angle Between Vertical and Horizontal Velocity Component. Depth 8.35 Meters, 21 October 1971.

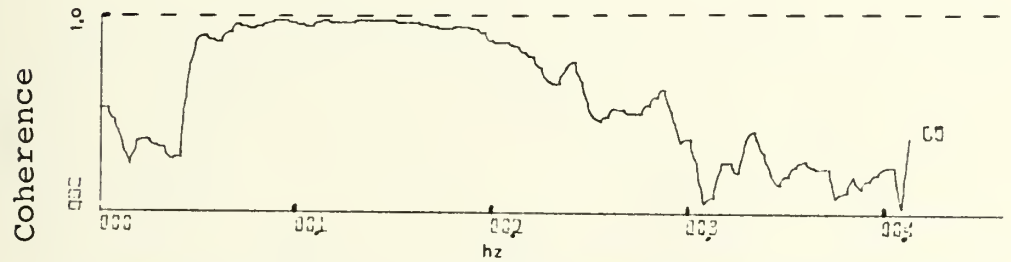

Coherence of Vertical and Horizontal Velocity Component. Depth 8.35 Meters, 21 October 1971.

Figure 23. Phase Angle and Coherence 8.35 Meters 21 October 1971.

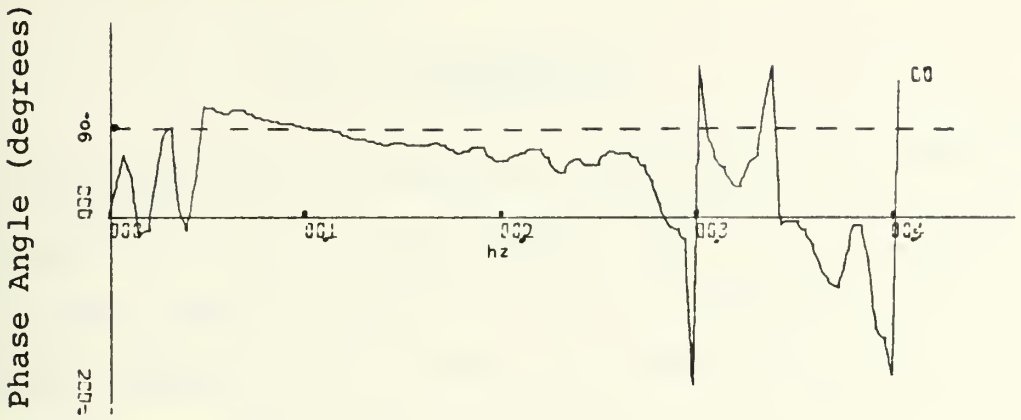

Phase Angle Between Vertical and Horizontal Velocity Component. Depth 10.00 Meters, 21 October 1971.

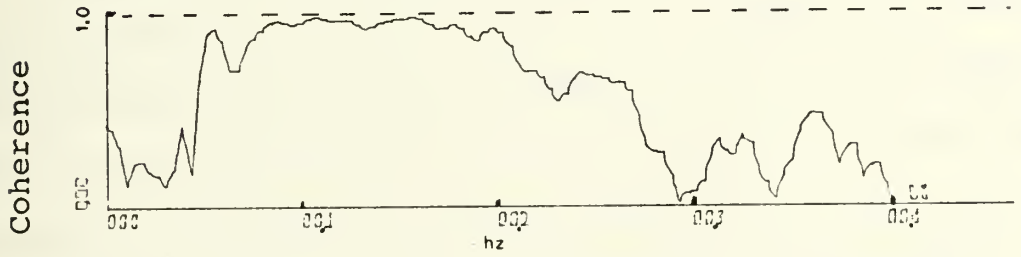

Coherence of Vertical and Horizontal Velocity Component. Depth 10.00 Meters, 21 October 1971.

Figure 24. Phase Angle and Coherence 10.00 Meters 21 October 1971.

VII. CONCLUSIONS

The measurements were made under near ideal conditions of moderate waves of low steepness and light wind conditions. A bi-modal swell was present during experiments with little locally generated wind waves. An electromagnetic flow meter having a response time corresponding to 2 Hz was used to measure water particle motion.

A. COHERENCE

Coherence of the wave height and orbital velocities was computed to be greater than 0.90 through the range of significant energy-density between 0.05 and 0.22 Hertz. This range contained greater than 90 percent of the total spectral energy-density which indicated that the water particle velocities were almost totally wave-induced. The high values of coherence obtained in all runs over the band of significant energy-density imply a near linear process between the wave height and induced orbital velocities. Under the moderate conditions encountered, non-linearities were small. Turbulent energy contribution to the energy-density spectra from both the sea surface and bottom boundary layer effects were quite small.

B. ENERGY-DENSITY SPECTRA

The energy-density spectra for the measured velocity at the four depths had approximately the same frequency bandwidth of significant energy-density. The shapes of

the measured and predicted energy-density spectra were approximately the same at each depth. The magnitude of the energy-density spectra decreased with depth according to theory.

C. PHASE ANGLE

The computed phase spectra of the wave height and wave-induced orbital velocities were consistent with theory in all cases except in the deepest run at 10.00 meters. The phase shift encountered in that instance was unaccounted for in the phase angle error analysis.

BIBLIOGRAPHY

Bendat, K. R. and A. G. Pierson, Measurement and Analysis of Random Data, pp. 234-237, Wiley, 1966.

Blackman, R. B. and J. W. Tukey (1959), The Measurement of Power Spectral, Dover Publication, Inc., New York, New York.

Bowden, K. F. and L. A. Fairbairn (1956), Measurements of Turbulent Fluctuation and Reynolds Stress in a Tidal Current, Royal Society of London Proceedings, Ser. A237 (1956), pp. 422-438.

Bowden, K. F. and R. A. White (1966), Measurements of the Orbital Velocities of Sea Waves and Their use in Determining the Directional Spectrum, Geophysical Journal of the Royal Astronautical Society, Vol. 12, 1966, pp. 33-54.

Inman, D. L. and N. Nasu (1956), Orbital Velocity Associated With Wave Action Near the Breaker Zone, U. S. Army Corp of Engineers, Beach Erosion Board, Technical Memorandum No. 79, March 1956.

Lynch, J. L. (1970), Long Wave Study of Monterey Bay, Naval Postgraduate School, Monterey, California, M.S. Thesis.

Miller, R. L. and J. M. Zeigler (1964), The Internal Velocity Field in Breaking Waves, 9th Conference on Coastal Engineering National Council for Wave Research, Lisbon, Portugal.

Nagata, Y. (1963), Observation of Wave Motion by Electromagnetic Current Meter, Proceedings Meeting on Coastal Engineering, Japan Society of Civil Engineering, 1963.

Nagata, Y. (1964a, 1964b), The Statistical Properties of Orbital Wave Motion and Their Application for the Measurement of Directional Wave Spectra, Journal of the Oceanographical Society of Japan, Vol. 19, pp. 169-181.

Seitz, R. C. (1971), Measurement of a Three-Dimensional Field of Water Velocities at a Depth of One Meter in an Estuary, Journal of Marine Research 1971, Vol. 29, pp. 140-150.

Simpson, J. H. (1968), Observation of the Directional Characteristics of Waves, Geophysical Journal of the Royal Astronautical Society, Vol. 17, 1969, pp. 93-120.

INITIAL DISTRIBUTION LIST

		No. Copies
1.	Defense Documentation Center Cameron Station Alexandria, Virginia 22314	2
2.	Library, Code 0212 Naval Postgraduate School Monterey, California 93940	2
3.	Oceanographer of the Navy The Madison Building 732 N. Washington Street Alexandria, Virginia 22217	1
4.	Department of Oceanography, Code 58 Naval Postgraduate School Monterey, California 93940	3
5.	Commander, Navy Ship Systems Command Code 901 Department of the Navy Washington, D. C. 20305	1
6.	Dr. Ned A. Ostenso Deputy Director (acting) Code 480 D Ocean Science and Technology Division Office of Naval Research Arlington, Virginia 22217	1
7.	Dr. Albert D. Kirwan, Jr. Program Director/Physical Oceanography Code 481 Ocean Science and Technology Division Office of Naval Research Arlington, Virginia 22217	1
8.	LCDR Jon W. Carlmark (USN) Project Office Code 485 Ocean Science and Technology Division Office of Naval Research Arlington, Virginia 22217	1

9. Professor H. Medwin, Code 61Md — 1
Department of Physics
Naval Postgraduate School
Monterey, California 93940

10. Asst. Professor Noel E. Boston, Code 58Bb — 1
Department of Oceanography
Naval Postgraduate School
Monterey, California 93940

11. Asst. Professor Edward B. Thornton, Code 58Tr (Thesis Advisor) — 5
Department of Oceanography
Naval Postgraduate School
Monterey, California 93940

12. Lieutenant Michael W. Bordy (USN) — 1
USS Implicit (MSO 455)
FPO San Francisco, California 96601

DOCUMENT CONTROL DATA - R & D

(Security classification of title, body of abstract and indexing annotation must be entered when the overall report is classified)

ORIGINATING ACTIVITY (Corporate author)
Naval Postgraduate School
Monterey, California 93940

2a. REPORT SECURITY CLASSIFICATION
Unclassified

2b. GROUP

REPORT TITLE
Spectral Measurements of Water Particle Velocities Under Waves

DESCRIPTIVE NOTES (Type of report and inclusive dates)
Master's Thesis, March 1972

AUTHOR(S) (First name, middle initial, last name)
Michael W. Bordy

REPORT DATE	7a. TOTAL NO. OF PAGES	7b. NO. OF REFS
March 1972	51	10

8a. CONTRACT OR GRANT NO.	9a. ORIGINATOR'S REPORT NUMBER(S)
b. PROJECT NO.	
c.	9b. OTHER REPORT NO(S) (Any other numbers that may be assigned this report)
d.	

10. DISTRIBUTION STATEMENT
Approved for public release; distribution unlimited.

11. SUPPLEMENTARY NOTES	12. SPONSORING MILITARY ACTIVITY
	Naval Postgraduate School Monterey, California 93940

13. ABSTRACT

Simultaneous measurements of the instantaneous sea surface elevation and water particle velocities were made using a wave staff and an electromagnetic current meter. Measurements were made at three elevations in 18 meters of water at an open ocean site during moderate wave and wind conditions. Coherence of the wave height and orbital velocities was computed to be greater than 0.90 through the range of significant energy-density between 0.05 and 0.22 Hertz. This range contained greater than 90 percent of the total spectral energy-density which indicated that the water particle velocities were almost totally wave-induced. Measured velocity energy-density spectra were compared to theoretically computed spectra using linear wave theory formulation. The measured spectra were 27 to 45 percent greater than theoretical spectra indicating that measured velocities were 5 to 7 percent greater than the theoretical values. Phase spectra were computed for the measured wave heights and orbital velocities. They compared reasonably with first order wave theory.

KEY WORDS	LINK A		LINK B		LINK C	
	ROLE	WT	ROLE	WT	ROLE	WT
wave orbital velocities						
energy-density spectra						
coherence						
phase angle						
electromagnetic current meter						